

Forti Luca (Orcid ID: 0000-0002-2965-9955)

Pezzotta Andrea (Orcid ID: 0000-0002-1093-1576)

**Declassified intelligence satellite imagery as a tool to reconstruct past landforms and surface processes. The submerged riverscape of the Tigris River below the Mosul Dam Lake, Iraq**

Luca Forti<sup>1,2\*</sup>, Guido S. Mariani<sup>3</sup>, Filippo Brandolini<sup>4</sup>, Andrea Pezzotta<sup>1</sup>, Andrea Zerboni<sup>1</sup>

<sup>1</sup>) Dipartimento di Scienze della Terra "A. Desio", Università degli Studi di Milano, via L. Mangiagalli 34, I-20133 Milano, Italy.

<sup>2</sup>) Istituto di Geoscienze e Georisorse, Consiglio Nazionale delle Ricerche, Via G. Moruzzi 1, 56124 Pisa, Italy.

<sup>3</sup>) Dipartimento di Scienze Chimiche e Geologiche, Università degli Studi di Cagliari, Italy.

<sup>4</sup>)McCord Centre for Landscape - School of History, Classics and Archaeology Newcastle University, Armstrong Building, Newcastle upon Tyne - NE17RU (UK)

**\*Corresponding author**

Luca Forti

Università degli Studi di Milano, Dipartimento di Scienze della Terra "A. Desio"

Via L. Mangiagalli 34, 20133 Milano, Italy

Phone: +393337173054

This article has been accepted for publication and undergone full peer review but has not been through the copyediting, typesetting, pagination and proofreading process which may lead to differences between this version and the Version of Record. Please cite this article as doi: 10.1002/esp.5389

E-mail: [luca.forti@unimi.it](mailto:luca.forti@unimi.it)

## **Acknowledgements**

Field survey in the region was conducted under the umbrella of the Italian Archaeological Mission to the Kurdistan Region of Iraq of the University of Udine directed by D. Morandi Bonacossi, who is kindly acknowledged. We are grateful to the General Directorate of Antiquities of the Kurdistan Regional Government, the Directorate of Antiquities of Dohuk, and the State Board of Antiquities and Heritage in Baghdad for granting all necessary work permits and their unremitting support. We greatly acknowledge the Editor S.N. Lane for valuable comments and support. Funding for analyses was provided by the Università degli Studi di Milano, Progetto Linea 2 (2017) and project CTE\_NAZPR19AZERB\_01 entrusted to A. Zerboni. Part of this research was supported by the Italian Ministry of Education, Universities, and Research (MIUR) through the project 'Dipartimenti di Eccellenza 2018–2022' (WP4 – Risorse del Patrimonio Culturale) awarded to the Dipartimento di Scienze della Terra 'A. Desio' of the Università degli Studi di Milano.

## **Author Contributions**

LF and AZ: Conceptualization, Methodology, Investigation, Writing – Original draft preparation, Visualization. GSM: Methodology, Writing – Original draft preparation. FB and AP: collaborate to data analyses and discussion. All authors approved the final version of manuscript.

## **Data Availability Statement**

The data sets used and/or analyzed during the current study are available from the corresponding authors on reasonable request

## **Abstract**

Located along the Tigris River in the Kurdistan Region of Iraq, the Mosul Dam reservoir is the second biggest dam of the Near East and represents an important water storage for local human activities. The dam was built between 1981 and 1988 north of the village of Eski Mosul, submerging the course of the Tigris River for ca 100 km. The analysis of historical images derived from declassified Corona satellite imagery acquired between December 1967 and August 1968 reveals the pristine pattern of the Tigris River, including the seasonal changes of its riverbed, shifting across the hydrological year from meandering to anastomosing patterns. Geomorphological mapping based on Corona images allowed to estimate the seasonal modification of fluvial elements such as the floodplain and point, middle, and longitudinal bars. The comparison with Landsat data collected since the 1990ies showed the first phases of the basin filling and the control on the present-day aspect of the lake inherited from the setting of the Tigris channel belt and, more in general, the litho-structural control over the evolution of the local hydrographic network; we also document the influence of the original Tigris River course on its recent insertion into the lake. Our work allowed reconstructing the ancient fluvial landscape below the Mosul Dam Lake and the evolution of its riverscape controlled by litho-structural factors and seasonal variations of the river discharge. Finally, this

contribution highlights the relevance of declassified intelligence satellite imagery in interpreting natural geomorphic processes and landforms today altered by human agency.

**Keywords:** Riverscape; Fluvial Geomorphology; Seasonality; Tigris River; Mosul Dam Lake; Iraq.

## 1. Introduction

Rivers are among the most dynamic environments in terms of landscape change and impact on human communities (Dollar, 2004; Charlton, 2007; Thorndycraft et al., 2008; Buffington and Montgomery, 2013; Tadaki et al., 2014; Jézéquel et al., in press). Their evolution depends on numerous factors, ranging from tectonics and climate to human intervention, often difficult to recognise as separate triggers and in many cases deeply modified by recent human agency (Brown et al., 2017; Tarolli et al., 2019). Remote sensing and field investigations on water courses and their surrounding landscapes can help in the reconstruction of the processes underlying fluvial evolution. This is especially true for arid regions, where the poor plant cover allows very precise and detailed observations even from remote (Perego et al., 2011). Moreover, in such contexts the effects of lithological and structural constraints are more immediate to be identified (Zerboni et al., 2020), greatly helping the formulation of more effective models.

Among the great rivers of the planet, the Tigris and the Euphrates are very important for the natural and human history of Mesopotamia, in the past as well as today. Their courses, from Turkey to the Gulf, is controlled for the most part by the structural evolution of the region, a quite active area of converging plates (Sissakian et al.,2020; Fouad et al., 2012; Al-Dabbagh and Al-Naqib, 2009; Al-Saigh, 2008). The Tigris River flows for 1800 km from the Taurus mountains in Turkey through the border with Iraq and then into the Gulf. Almost 56% of its basin lies in Iraq, with 6 major tributaries and secondary rivers draining most of the runoff from the Iraqi mountainside of the southern Zagros. The Tigris River is less meandering than the Euphrates, and along many of its branches, especially after the Iraq-Turkey border, its course is strongly influenced by the geodynamic setting of the Arabian-Eurasian plate convergence. In modern times, the course of the Tigris River has been constrained in multiple places by human action through the construction of dams, which greatly modified the local landscape and flooded several villages and archaeological sites (ESCWA, 2013; Sconzo and Simi, 2020; Titolo, 2021). At the same time, new artificial basins show non-homogenous aspects, which probably follow previous natural constraints, ultimately related to the settings of the ancient course of the Tigris River. In the contexts of artificial lakes, despite the arid climate and the low plant cover allowing a very good visibility of ground features, it is hard to map landforms and interpret the factors triggering the evolution of fluvial landforms since a relevant portion of the landscape is submerged and invisible to field observation.

To overcome this issue, in the present work we combine geological and geomorphological data with the observations of declassified satellite images collected before the construction of the Mosul Lake Dam (MLD), thus representative of the pristine local riverscape. Such multi-temporal mapping approach (Zerboni et al., 2020) aims to: (i) reconstruct the ancient course of the Tigris River upstream of Mosul, (ii) describe its seasonal dynamics before the construction of the dam, and (iii) correlate the current dynamic of the lake to lithological and structural factors that in the past may have controlled the development of the river. The use of a multidisciplinary approach permitted to reconstruct the submerged riverscape of the Tigris River, showing the underlying causes that shaped fluvial dynamics as much as the current lake and helping in the reconstruction of past geomorphic processes. Finally, we highlight the relevance of declassified intelligence satellite imagery as a tool to interpret the dynamic of past geomorphic processes and landforms today influenced/altered/obscured by human agency.

## **2. The study area**

### **2.1. Geological and climatic background**

The study area covers 1250 km<sup>2</sup> of the north-western Kurdistan Region of Iraq (KRI) in the governorates of Dohuk and Nineveh (Fig. 1). The landscape is the result of the interplay between geological-structural, geomorphological and climate-driven processes (Forti et al., 2021), and

subsequently the construction of Dam and its infilling in the '80ies (Adamo and Al-Ansari, 2016).

The area is in the Low Folded Zone, within the Outer Platform of the Arabian Plate part of the Zagros-Fold Thrust Belt (ZFTB; Fouad, 2007). This structure is the result of the collision between the Arabian and Eurasian continental plates that started in the Early Miocene and is still actively progressing today (Dercourt et al., 1986; Fouad et al., 2012; Mouthereau et al., 2012; Csontos et al., 2012). Low-elevation mountains and lowlands characterise the area. Their distribution is controlled by the presence of anticline ridges, mainly oriented W-E (Ain Zala, Zainiyat, Butma, Ravan, Dohuk, Dakhan, Masra and Kand anticline) (Fig.1; Figs.2a-b) and NW-SE (Mashura Dag, Sufiya and Baikhair) (Fouad et al., 2012; Abdulnaby, 2019) and by the NW-SE development of the Dohuk Fault System (*sensu* Al-Dabbagh and Al-Naqib, 2009; Al-Saigh, 2008, 2012) with the main alignment of the Sasa-Bekhair Fault (Fouad et al., 2012; Sissakian et al., 2018).

The anticline ridges are mainly composed by Paleocene to Lower Miocene limestone and dolostone, whereby in the Mosul Lake area the anticline is characterized by the Miocene to Mio-Pliocene Fatha, Injana and Mukdadiyah Formations, alternating marl and gypsum with sandstone and limestone (Sissakian and Fouad, 2012) (Fig.1; Fig. 2d). Plio-Pleistocene conglomerates outcrop along the northern banks of Mosul Lake and in the proximity of the dam (Fig. 2c) (Al-Dabbagh and Al-Naqib, 1991; Sissakian and Al-Jibouri, 2012).

Quaternary deposits are mainly located along the hillslopes of anticlines and in the lowland areas of the syncline troughs. They include fluvial, floodplain, alluvial fan, colluvial, and anthropogenic deposits (Jassim and Goff, 2006; Sissakian and Al-Jibouri, 2012, Forti et al., 2021). Quaternary deposits are composed by conglomerates with fine to coarse sand, with levels of silt and clay recognized at different locations of the area, especially on the fluvial terraces above the banks of the Tigris River (Al-Dabbagh & Al-Naqib, 1991). Such deposits are eroded and reworked by the action of the fluvial network draining from NE into the Mosul Lake to the SW.

Climatic data for the study area derive from a meteorological station placed in the cities of Mosul and Dohuk and were elaborated for climate models by Awchi and Kalyana (2017) and Sulaiman (2016). Models suggest that the Mosul Lake is located between two climatic zones of the climate classification proposed by Köppen and Geiger (1936). The first zone is the Mediterranean or Dry Summer Subtropical (Csa), while the second one is Subtropical Steppe (Bsh) (Salman et al., 2019; Malinowski, 2002). The Csa climatic zone in this area is characterized by extremely to moderately cold wet winters and moderately hot arid summers. Precipitations occur during the winter and spring seasons from November to April with an estimated mean rainfall at Dohuk station of 570 mm and seasonal temperature variations from 8.8°C to 34 °C (Awchi and Kalyana, 2017; Sulaiman, 2016; Malinowski, 2002). The Bsh climate zone has moderately cold winters and hot to extremely hot dry summers. Long-term climate data extrapolated from the Mosul meteorological station (Awchi and Kalyana, 2017) show that

most rainfall occurs during the winter season and the annual mean rainfall from 1937 to 2010 is 378 mm. Annual mean temperature is 21°C with extremely hot summers with mean temperatures of around 40°C.

Most rivers in the region are ephemeral, active during the rainy season (Othman and Gloaguen, 2013) and inactive in the dry season; only the Tigris River and a few of its tributaries are perennial. Several climate models showed a strong increase of drought events in recent times. From the 1980ies to 1990ies the area surrounding the Mosul Lake suffered several periods of drought. At the beginning of the 1990ies and especially in the last decades of the 20<sup>th</sup> century, severe droughts are recorded (Al-Khafaji and Al-Ameri, 2021; Alwan et al., 2019; Awchi and Kalyana, 2017). In addition to climate change, the dam's water supply has been threatened by ongoing conflicts in the area over the past four decades (Hasan et al., 2019).

## **2.2. Hydrological setting of the Tigris River and the Mosul Lake Dam**

The Tigris River originates in Turkey along the southern slope of the Taurus mountains (Altinbilek, 2007). The river flows through Turkey, Syria, and Iraq. After 1800 km the Tigris River merges with the Euphrates River in the South of Mesopotamia, forming the Shatt-Al-Arab River that flows into the Gulf, 220 km downstream (Fig. 3a).

The main tributaries from Iraq and Syria are the Feysh Khabur, Great Zab, Lesser Zab, Adhaim, and Diyala Rivers. The Feysh Khabur River joins the Tigris River west of the municipality of Zacko, while the Great Zab and

Lesser Zab Rivers respectively to the SE of the cities of Mosul and Fatha. The Adhaim and Diyala River merge into the Tigris River south of Fatha and in the proximity of Baghdad; afterwards, no major tributary rivers are recognized except for a few agricultural canals draining from the Zagros piedmont in the internal floodplain of the Tigris River. The Tigris River drainage basin occupies a total area of  $\sim 221,000 \text{ km}^2$ , for the 60% in Iraq territory; its mean discharge at Mosul city was  $700 \text{ m}^3/\text{s}$  in 1984 and dropped to  $596 \text{ m}^3/\text{s}$  after the construction of the dam. The overall amount of the Iraqi catchment area is  $\sim 124,000 \text{ km}^2$ ; the annual mean discharge changes according to the Tigris setting and the minor tributary basins to the South (Fig. 3 b, c) (Saleh, 2010; Al-Ansari and Knutsson, 2011; Al-Ansari, 2013; ESCWA, 2013).

The MLD is the largest dam in Iraq and one of the biggest of the Near East with a storage capacity of  $11.11 \text{ km}^3$  of water (Al-Ansari et al., 2015). It is 3650 m in length and 113 m high with an embankment core composed by clays. It was built to provide water for irrigation, control floods, and hydropower generation (Fig. 4). During the preparation of the site for construction operations, problems related to grouting work on the foundations of the dam were recognized. In fact, the geological bedrock of the dam consists of gypsum, marl, and limestone layers interbedded with breccias which are intensely fractured by the Dohuk Fault System, allowing seepage and karst processes to act on the stability of the dam (Al-Dabbagh and Al-Naqib, 2009; Al-Saigh, 2008, 2012; Sissakian et al.,

2014). Construction works started in January 1981, and the dam became operational in July 1986.

### **3. Materials and methods**

To investigate the recent evolution of the Tigris River and its riverscape in the area submerged by the MLD, including the major factors controlling its development, we performed a detailed geomorphological mapping of the area and an analysis of its seasonal changes.

Geomorphological mapping of the area was performed on data interpreted from both declassified Corona, Landsat, Sentinel 2A/2B, Esri World Imagery, Bing Virtual Earth and GoogleEarth™ satellite images (Bing Maps, 2021; Esri, 2021) (Fig.5). Declassified Corona satellite image dataset was downloaded from CAST Atlas of the University of Arkansas (<https://cast.uark.edu/research/corona.php>) (USGS, 1968); in particular, we considered December 1967 (1102-1025) and August 1968 (1104-2138) images. Landsat and Sentinel 2 were selected from the EarthExplorer platform of the USGS (<https://earthexplorer.usgs.gov>) and cover a period from June 1984 to August 1986 and March and July 2016-2020. We used 11 declassified Corona, 15 Landsat and 11 Sentinel-2 images (Table 1). Landsat and Sentinel-2 imagery was observed in false colours (red = band 4, green = band 3, blue = band 2). Corona imagery was observed in single band grayscale.

Corona images helped in mapping landforms to understand their seasonal geomorphic shift (Gilvear and Bryant, 2016; Gurnell et al., 2016). The

mapping considered different geomorphic units, illustrating the effect of fluvial, slope, and anthropogenic processes. Fluvial geomorphic units are the most important for our study and were described to highlight seasonal changes in the fluvial pattern; we adopted the classification proposed by Brierley and Fryirs (2013). Landsat images taken from 1984 to 1986 were used to emphasize the time and steps of the infilling of the MLD. Moreover, true colour GoogleEarth™, Bing Virtual Earth and Esri World Imagery images were used to investigate the influence of the ancient river planform of the Tigris River on the present setting of the Mosul Lake. The choice of specific dates for Sentinel-2A/2B imagery is based on known operations and discharge variations for 2016, 2019, and 2020, as they were used for detecting seasonal fluctuations of lake shorelines controlled by variations in the discharge of the Tigris and seasonal dam operations. We reconstructed the discharge for the Tigris River ca. 20 years before the start of the construction of the dam, namely for the period between December 1967 and August 1968 (declassified Corona satellite imagery). The same was done for the period between 1984 and 1986 during the filling steps of the basin (Landsat imagery).

Remote sensed images were projected in the UTM Zone 38 reference system and used as the background for remote observations in QGIS 3.16 software. Also, Digital Elevation Model (DEM) MERIT with 3 arcsec horizontal resolution (~90 m at the equator) was projected in the UTM Zone 38 and used to extrapolate the Tigris and tributaries watershed (Yamazaki et al., 2017). The geological bedrock and main linear structural features

were extracted from the of Al-Mosul Quadrangle geological map (1:250,000) of the Series of the Geological Map of Iraq (Ministry of Industry and Minerals, Iraq Geological Survey, 1995; 1997; 2014) and from the Tectonic Map of Iraq (Fouad, 2012); additional structural data come from Al-Saigh (2008), Al-Dabbagh and Al-Naqib (2009), and Sissakian et al. (2018).

## **4. Results**

### **4.1. Geomorphological variability of the Tigris riverscape before the MDL**

The comparison between declassified Corona imagery from December 1967 and 1968 revealed several changes in the river planform, including variations in the setting of mid-channel and bank-attached landforms. In response to the seasonal variation of discharge (meant as flow stage), the behaviour of the river, or at least of some of its parts, starts to adjust and re-equilibrate erosional and depositional processes (Fig. 5).

The relationship between discharge variations and river pattern are strongly connected with the lithological and structural setting in which the Tigris River flows. In the study area, the Tigris River changes between different structural settings, which are ultimately related to the effects of the evolution of the local anticline-syncline system and the Dohuk Fault System. In fact, the anticline-syncline system influenced the ability of the river to cut into the bedrock and thus the width of its valley. Consequently, the Tigris River below the MDL shifts from partly confined to unconfined

and the river planform is not homogeneous. Also, these elements impact on the shape and width of the floodplain and its related geomorphic units.

#### **4.2. Geomorphological mapping of the winter season**

The declassified Corona imagery taken on 11 December 1967 recorded the Tigris River at its bank full stage. At that time, the monthly mean discharge at streamflow-gaging station of Mosul was 481.40 m<sup>3</sup>/s. The main recognizable features are fluvial landforms related to the active channel stream point and the mid-longitudinal bars. On the banks of the active channel a sequence of three levels of terraces is visible (T1, T2 and T3, oldest to youngest) (Fig.2c). Some reach banks of the Tigris River show an erosional scarp caused by undercutting and gravity collapse. Floodplains are in the proximity of the sinuous reach of the Tigris River; most of them display active chute channels and meander scars with traces of paleochannels. The latter were exploited for cultivation. Moreover, secondary tributaries are mainly distributed along the left bank of the Tigris; they flow along the erosional pediment that connects the anticline slope to the river (Fig. 6).

The lithological and structural setting of the bedrock affected the morphodynamics of the Tigris River, but also influenced the other geomorphological processes acting in its proximity. A homogeneous belt of flatirons is visible on anticline hills; minor streams also dissect the hillsides creating badlands upon marls, gypsum, and conglomerate outcrops.

South of the dam site, a landslide body and its denudation surface occur; the curved geometry of the foot of the deposit modifies the course of the Tigris River forcing the development of an irregular meander.

### **4.3. Geomorphological mapping of the summer season**

The declassified Corona images taken on 16 August 1968 capture the Tigris River during a phase of low flow stage. The monthly mean discharge recorded at the streamflow-gaging station of Mosul was 211.60 m<sup>3</sup>/s. Compared with the winter season, the general landscape of the area does not show evident changes. On the other hand, within and along the main course of the Tigris River visible variations appear. The low water level exposes several mid-channel and bank-attached geomorphic features, which reflect the variety of landforms – and related processes – that changed during the seasonal fluctuation of discharge (Fig. 7).

The main mid-channel geomorphic units recognized relate to the width of the channel and to the type and shape of the planform in which they developed. In the northern part of map, the river shows a decrease in the number of channels in which it flows. A single channel with low sinuosity and few meanders shifts to a course with multiple meanders and up to three channels. In general, compound and point bars occur on the convex banks of tortuous meander bends (Fig. 8a). Bars are covered by ephemeral vegetation with slack water confined in chute channels and in the scours. Downstream, asymmetrical lateral bar, scroll bars, and mainly mid-channel bar units form along the low sinuosity reach (Figs. 8b, c). The mid-channel

units are composed by raindrop shaped longitudinal bars, elongated along the direction of the flow, and by diagonal bars, oval to sigmoidal in shape and oriented perpendicularly to the channel banks (Brierley and Fryirs 2013) (Figs. 8d, e). Vegetated mid-channel islands are strictly connected to the channel dynamics, reflecting the river storage capacity for sediments (Brierley and Fryirs 2013) (Fig. 8e). This is, in turn, related to how processes reshaped the river course before and after flood events: in fact, during its low flow stage the Tigris River displays a multiple channels pattern only where mid-channel islands and compound bars occurred (Fig. 8f)

#### **4.4. Factors controlling the Tigris riverbed landscape**

Reconstructing the landscape of the Tigris River before the filling of the Mosul Dam reservoir revealed the main factors that influenced the pattern and planform of channels over time. The different effects of lithology, geological structure and river behaviour allow to divide the area into three zones: upstream, middle-stream and downstream. These are treated separately to better expose the influence of each factor on the diversity of channel shapes.

##### **4.4.1. Upstream lithological controls**

The upstream river planform of the Tigris River is ca. 43 km long and different river planforms are visible during the bankfull (1967) and low flow stages (1968) (Fig. 9a). From NW towards SE the Tigris River changes its

sinuosity. The first portion of the stream is characterised by tortuous meanders with small point bars and two/three terrace levels; small floodplain pocket can also sometimes develop when the river course is partly confined inside a narrow valley. Afterwards, the number of channels increases, and the river setting shifts from a wandering to an anabranching gravel bed according to the flow stage (Figs. 9b, c). A wide floodplain with meander scars, chute channels, paleochannels, and superimposed agricultural fields characterizes the right bank. On the 1967 Corona image, this part of the river shows a pathway of flood channels active during high discharge events. The shape of mid-channel and bank attached geomorphic units varies in both 1967 and 1968. In this portion, the major constrain on the Tigris River dynamic is the lithological change of the bedrock from the marls and sandstones of the Injana and Fatha formations to the Plio-Pleistocene conglomerates (Fig. 9d). The latter increases the size of the bed material with coarse grained sand and pebbles. These materials form river islands, flooded during high discharge flows and exposed and covered by vegetation in the low flow stage. The island plant cover ensures the stability of each bar: while the action of erosional and depositional processes can modify their shape with time, they never shift from their original location.

#### **4.4.2. Middle-stream channel shape change**

The middle-stream is 45 km long and is characterized by a decrease of the braiding degree and a correspondent increase in sinuosity of the channel planform (Fig. 10a). The uppermost part of this section follows a meandering pattern with point bars migrating northwards. More downstream, the low sinuosity reach hosts a small pocket floodplain with bank attached and mid-channel geomorphic features such as longitudinal, lateral, and compound bars. Afterwards, two tortuous meanders develop in a confined to partly confined valley; here are visible a compound point bar and an encased convex bend with a scroll bar in the concave zone. In the lowest portion, the river planform changes into an irregular straight planform with lateral bars in the bankfull stage attached at the riverbanks during low flow stage (Figs. 10b, c). The evolution of this part of the river was influenced by the structure of the anticline ridges of Ain Zala, Ravan, and Zainaiyat and by the effects of Dohuk Fault System driving the development of encased meanders into the marl bedrock of the Fatha Formation (Fig. 10d).

#### **4.4.3. Downstream and Dam site diversity**

The downstream portion of the Tigris River occupies the last 20 km before the dam site. The river follows a tortuous planform flowing in a partly confined valley setting; wide floodplains form in the inner bend of two meanders and along the left bank of the last straight part of river before the dam site (Fig. 11a). At the low flow stage, lateral bars and compound

bars with point bars occur. A series of floodchannels and a wide floodplain occupied by cultivations is visible in the inner part of the point bar, located in the last meander. The floodplain before the dam site is crossed by secondary little branches of the Tigris. During bankfull flow stage, such geomorphic features are submerged and affected by erosional and depositional processes which change their shape and dimensions (Figs. 11b, c).

#### **4.4.4. Examples of variations of riverbed and mid-channel to bank-attached geomorphic features**

The comparison between declassified Corona images reveals differences in the behaviour of the Tigris River planform and its related geomorphological features. Two examples from the upstream portion help in explaining how the Tigris channel belt adjusted to seasonal discharge fluctuations.

In the first example, the Tigris River flows in a partly confined valley forming a meandering planform; this area is characterized by floodplains and neck cut-offs. In the low flow stage, the meanders are partly interconnected and filled by water (Fig. 12a). During the bankfull stage, a large meander is instead connected to the main Tigris River channel, with the formation of an island covered by vegetation and crossed by a flood channel network (Fig. 12b).

The second example shows the effect of the switch in planform geometry caused by the transition from a fine- to a coarse-grained channel bedload.

There, the seasonal change from bankfull to low flow stage triggered the shift of many channels from wandering to anabranching (Figs. 12c, d).

#### **4.5. The filling of the Mosul Dam reservoir (1984–1986)**

The filling phases of the Mosul Dam reservoir are reconstructed through the comparison of a selection of Landsat images acquired from 1984 to 1986. Such reconstruction reveals the first impact of the barrage operations on the Tigris River. In 1984 and 1985, the Tigris River was progressively dammed with an embankment made by a core of silt and clay (Figs. 13a–d). At this stage, the shape of the incipient lake in the first area subjected to inundation followed the inherited fluvial landform and valley setting of Tigris River. According to our analysis, the first inundated zones (inundation occurred between the end of 1985 and the beginning of 1986) were the lowlands and the floodplain located near the Mosul Dam site due to the laterally unconfined setting (Fig. 13e). Subsequently, upstream migration flooding affected the middle and upstream area, in the meandering and floodplain locations towards NW in partly confined and unconfined valley settings (Figs. 13f, g). The final filling of the reservoir took one year, between June 1985 and July 1986 (Figs. 13h, i). The impact on the 1986 annual discharge was important: it was estimated as only 269,88 m<sup>3</sup>/s, against 546.00 m<sup>3</sup>/s of 1984, 624,57 m<sup>3</sup>/s of 1985, and later 877,93 m<sup>3</sup>/s of 1987 (Saleh,2010).

The impact of the extremely rapid filling phases of the MDL was not confined on the Tigris riverscape; this event also triggered several changes onto the

local morpho-structural setting around the dam site and the surrounding area. In fact, an increase in local seismic activity was recorded as a swarm of micro-earthquakes between 1986 and 1987; Al-Saigh (2008) suggests that micro-earthquakes were triggered by the large volume of water in the reservoir.

The construction of the dam also affected the aquifers hosted in the bedrock of the dam site increasing the circulation of groundwater in strata of gypsum with breccias (Fatha Fm.). As a result, the rate of karst dissolution of the bedrock increased dramatically. In fact, monitoring surveys of the area after 1985-1986 revealed the development of sinkholes and dolines in proximity of the dam, which also affected the stability of the dam itself (Al-Dabbagh and Al-Naqib, 2009; Al-Saigh, 2008; Kelley et al., 2007).

## **5. Discussion**

### **5.1. Variations of the Tigris planform and litho-structural control**

The mapping of the seasonal riverscape of the Tigris River obtained from the analysis of winter and summer Corona images allow to reconstruct the behaviour of a part of the river today submerged below the MDL. Our results highlight the litho-structural control over the fluvial pattern and the ability of the river to adjust its course during the low and high flow stages. Seasonal variations of the river discharge switched the processes of sedimentation and erosion, continuously reworking geomorphological features such as middle and point bars. Our observations suggest that local lithology and tectonic settings are the major factors influencing fluvial

dynamics, especially for valley setting, slope evolution, sedimentary budget, and the general flow direction of the Tigris River (Fig. 14a).

Upstream to downstream, it is possible to observe how the Tigris plan morphology changes according to the constraints imposed by these factors.

The upstream area shows a meandering pattern with tortuous meanders switching from wandering (low flow stage) to anabranching (high flow stage) (Fig. 12c, d); this pattern corresponds to areas with a bedrock composed mainly by marls and conglomerates (Fig. 9d). The river behaviour influences the distribution and organization of bars downstream with the formation of small point and middle bars, and of a gravel bed with transversal bars and plant-covered islands.

Further downstream, the shape and flow direction of the middle- and downstream portions are driven by the structure of anticline ridges and the activity of the Dohuk Fault System. Here, the direction and fluvial plan geometry of four distinct reaches clearly follow the strike direction of the anticlines and the Dohuk Fault System (Fig. 14b). In the first portion, the Tigris River follows the general direction of the Ain Zala Anticline (Fig. 14c); here the position of faults controls the downstream increase in sinuosity of the channel to the development of a tortuous meandering course with point bars (Fig. 14d). Afterwards, the occurrence of the Ravan anticline triggers a river planform response, changing into an irregular straight planform with lateral bars; here the Tigris River generally flows parallel to the anticline ridge (Fig. 14e). Before the dam, in the downstream portion of the river, the impact of the syncline and of the Dohuk Fault System on the shape,

flow direction, and geomorphic dynamics of the Tigris is more evident. When the river reaches the subsidence area related to the syncline, the degree of sinuosity increases. Also, two meanders, a wide floodplain, and fluvial bars in different discharge settings appear (Fig. 14f). In the area closest to the dam, the presence of the fault system drives a decrease in sinuosity and a change in the direction of the Tigris flow, that shifts from NW–SE to NE–SW.

## **5.2. Control of the ancient Tigris riverscape over the shape of the MDL**

The actual shape of the MDL reservoir is the result of the interplay between the ancient Tigris riverscape, the litho-structural setting of the area, and the dam post-filling operations (Fig. 2a, b).

During filling operations, the MDL shoreline varies especially between March and July (Ahmed et al., 2012; Khattab and Merkel, 2014; Khattab et al., 2017; Leabi et al., 2020). Sentinel-2 images in March and July 2016 and 2020 record these variations of lake shorelines, especially in the upstream and downstream portions of the newly formed lake (Fig. 15). Shoreline variations are linked to the seasonal discharge of the Tigris as evidenced by data from the Ministry of Water Resources of Iraq (Leabi et al., 2020). Dam operations have a relevant impact on the variations of the lake level; for instance, shorelines periodical change in response to the seasonal drop of lake level permit to recognize some submerged archaeological sites that emerged during phases of seasonal drop of lake level (Titolo, 2021).

In this scenario, the morphology of the MDL appears to be strongly connected with the ancient geomorphological setting of the Tigris (Fig. 16a). The morphology and shoreline of the northern area (upstream), relates to the development of the old meander planform with the formation of a huge floodplain with neck and chute cut-off processes in a partly unconfined setting. This framework influences the inlet processes of the Tigris, both during flood events and in low flow stages when a deltaic plain appears (Fig. 16b). Afterwards, the narrowing of the lake is due to the same Plio-Pleistocene conglomerate bedrock which turned the course of the Tigris River from a wandering to anabranching planform with the formation of plant-covered bars.

The central part of the MDL (middle Tigris River stream) is characterized by a partly straight, partly arcuate coastline profile on the right banks. The complex structural setting of this portion strongly influences the lake shape in the same way as it did with the ancient Tigris River, which displayed a semi regular meandering planform in a partly confined setting with the development of compound and middle-longitudinal bars. The connections between the ancient Tigris, the structural setting, and the present lake morphology are visible in the subangular shape of the right banks and in the left tributary derived from the Dohuk Lake and driven by the Dohuk Fault System (Fig. 16c).

In the proximity of the dam, the reservoir reaches the maximum surface expansion due to the presence of a wide flat area formed by the interplay between the irregular growth of anticlines and the development of a

syncline trough, in which the meandering ancient Tigris River created compound point bars and a floodplain (Fig. 16d, Fig. 2a).

## **6. Conclusions**

The geomorphological investigation of the submerged riverscape of the Tigris River along the MDL permitted to reconstruct the dynamic of the river where it is no longer visible, and to identify the main hydrological and geomorphological changes regulated by seasonal variations of the discharge. Moreover, we were also able to correlate the evolution the Tigris River in response to litho-structural forcing that controlled the size and direction of its course. In fact, variations in the competency of the geological bedrock and the growth of geological structures (faults and folds) resulted in a complex riverscape that – along a relatively short part of the river – alternates confined and un-confined valleys, straight and meandering courses, anabranching to wandering settings. The same factors play an indirect control over the shape of the MDL; in fact, we identify an overprint of the submerged Tigris River riverscape on the present-day reservoir that is ultimately related to the major litho-structural forcing factors.

In a more general perspective, our approach confirms the reliability of historical declassified intelligence aerial/satellite pictures in geomorphological studies. In fact, historical remote data, as the declassified Corona, have a quite high resolution and, especially, permit to investigate regions in many cases not accessible and/or where intense

urban expansion and human agency have disrupted the natural landforms and altered pristine surface processes, thus reconstructing the pre-anthropogenic geomorphic dynamic. The case study of the MDL is emblematic because the building of the dam and the infilling of the reservoir completely changed the dynamics of natural processes and shrouded pristine landforms. Such example could help in investigating other regions where less invasive events may have impacted the natural systems modifying surface processes and the dynamics of the Earth Critical Zone. The comparison of present geomorphic settings with historical aerial/satellite imagery, as much as the use of historical maps, may reveal in detail the impact of the onset of human agency on landscapes in the last few centuries, shedding light on the effect of the Anthropocene on geomorphic surface processes.

## References

- Abdulnaby, W. (2019) Structural geology and neotectonics of Iraq, northwest Zagros. *In Developments in structural geology and tectonics*,3, 53-73
- Adamo, N. and Al-Ansari, N. (2016) Mosul dam full story: Safety evaluations of Mosul dam. *Journal of Earth Sciences and Geotechnical Engineering*, 6(3), 185-212. Available at:  
<http://urn.kb.se/resolve?urn=urn:nbn:se:ltu:diva-15334>
- Adamo, N., Al-Ansari, N., Issa, I., Sissakian, V. and Knutsson, S., (2015). Mystery of Mosul Dam the most dangerous dam in the world: maintenance grouting. *Journal of Earth Sciences and Geotechnical Engineering*, 5(3), 71-77. Available at:  
<http://urn.kb.se/resolve?urn=urn:nbn:se:ltu:diva-9410>
- Adamo, N., Al-Ansari, N., Sissakian, V., Laue, J. and Knutsson, S. (2019) Mosul Dam: Geology and Safety Concerns. *Journal of Civil Engineering and Architecture*, 13(3), 151-177. Available at:  
[10.17265/1934-7359/2019.03.001](http://dx.doi.org/10.17265/1934-7359/2019.03.001)
- Al-Ansari, N. (2021) Topography and Climate of Iraq. *Journal of Earth Sciences and Geotechnical Engineering*, 11, 1-13. Available at:  
<https://doi.org/10.47260/jesge/1121>
- Al-Ansari, N.A. (2013) Management of Water Resources in Iraq. *Perspectives and Prognoses. Engineering*, 5, 667-668. Available at:  
<http://dx.doi.org/10.4236/eng.2013.58080>

- Al-Ansari, N.A. and Knutsson, S. (2011) Toward Prudent Management of Water Resources in Iraq. *Journal of Advanced Science and Engineering Research*, 1, 53-67. Available at:  
<http://urn.kb.se/resolve?urn=urn:nbn:se:ltu:diva-11050>
- Al-Dabbagh, T.H. and Al-Naqib, S.Q. (1991) Tigris River terrace mapping in northern Iraq and the geotechnical properties of the youngest stage near Dao Al-Qamar village. *Geological Society, London, Engineering Geology Special Publications*, 7(1), 603-609.
- Al-Dabbagh, T.H. and Al-Naqib, S.Q. (2009) The Impact of Some Geologic Structural Elements on Fuse Plug South-eastern Alignment of Mosul Dam. *Iraq Journal of Earth Science*, 9(2), 27-38.
- Al-Khafaji, M.S. and Al-Ameri, R.A. (2021) Evaluation of drought indices correlation for drought frequency analysis of the Mosul dam watershed. *In IOP Conference Series: Earth and Environmental Science*, 779 (1)
- Al-Saigh, N. (2008). Seismicity of Mosul dam reservoir. *Iraqi National Journal of Earth Sciences*, 8(2), 11-16. Available at:  
<https://doi.org/10.33899/earth.2008.5481>
- Al-Saigh, N. (2012) Seismicity of Mosul Dam Reservoir for the Monitoring Year 1990. *Iraqi National Journal of Earth Sciences*, 12(1), 17-22. Available at: <https://doi.org/10.33899/earth.2012.36078>
- Altinbilek, D. (2004) Development and management of the Euphrates–Tigris basin. *International Journal of Water Resources*

*Development.*,20(1), 15-33. Available at:

<https://doi.org/10.1080/07900620310001635584>

Alwan, I.A., Karim, H.H. and Aziz, N.A. (2019) Agro-climatic zones (ACZ) using climate satellite data in Iraq republic. In IOP conference series: Materials Science and Engineering IOP Publishing.

Al-Zuhairi, M.F., Al-Jumaily, K.J. and Al-Salihi, A.M. (2016).

Characteristics of precipitation systems over Iraq observed by TRMM radar. *American Journal of Engineering Research*, 5(11), 76–81.

Awchi, T.A. and Kalyana, M.M. (2017) Meteorological drought analysis in northern Iraq using SPI and GIS. *Sustainable Water Resources Management*, 3(4), 451-463.

Bing Maps. (2021). Bing Maps. [online] Available at:

<<https://www.bing.com/maps>> [Accessed 5 November 2021].

Brierley, G. J. and Fryirs, K. A., (2013) *Geomorphology and river management: applications of the river styles framework*. John Wiley & Sons.

Brown, A.G., Tooth, S., Bullard, J.E., Thomas, D.S., Chiverrell, R.C.,

Plater, A.J., Murton, J., Thorndycraft V.R., Tarolli, P., Rose, J.,

Wainwright, J., Downs P. and Aalto, R. (2017). The geomorphology of the Anthropocene: emergence, status and implications. *Earth*

*Surface Processes and Landforms*, 42(1), 71-90. Available at:

<https://doi.org/10.1002/esp.394>

Charlton, R. (2007) *Fundamentals of Fluvial Geomorphology*. Routledge.

Csontos, L., Sasvári, Á, Pocsai, T., Kósa, L., Salae, A. T. and Ali, A.

(2012) Structural evolution of the northwestern Zagros, Kurdistan region, Iraq: Implications on oil migration. *GeoArabia*, 17, 81–116

Dercourt, J., Zonenshain, L.P., Ricou, L.E., Kazmin, V.G., Le Pichon, X.,

Knipper, A.L., Grandjacquet, C., Sbertshikov, I.M., Geysant, J.,

Lepvrier, C., Pechersky, D.H., Boulin, J., Sibuet, J.C., Savostin, L.A.,

Sorokhtin, O., Westphal, M. and Bazhenov, M. L. (1986) Geological

evolution of the tethys belt from the atlantic to the pamirs since the

LIAS. *Tectonophysics*, 123(1-4), 241–315. Available at:

[https://doi.org/10.1016/0040-1951\(86\)90199](https://doi.org/10.1016/0040-1951(86)90199)

Dollar, E.S.J. (2004) Fluvial geomorphology. *Progress in Physical*

*Geography: Earth and Environment*, 28(3), 405-450. Available at:

doi:10.1191/0309133304pp419pr

Eklund, L. and Seaquist, J. (2015) Meteorological, agricultural, and

socioeconomic drought in the Duhok governorate, Iraqi Kurdistan.

*Natural Hazards*, 76(1), 421–441. Available at:

<https://doi.org/10.1007/s11069-014-1504-x>

ESCWA (Economic and Social Commission for Western Asia),2013.

Inventory of Shared Water Resources in Western Asia. Salim

Dabbous Printing Co., Beirut, 626 p.

ESRI, (2021) "World Imagery [basemap]. "World Imagery". July 22,

2020.

<http://www.arcgis.com/home/item.html?id=10df2279f9684e4a9f6a7f>

08febac2a9 (accessed 11/11/2021).

Forti L., Perego A., Brandolini F., Mariani G.S., Zebari M., Nicoll K.,  
Regattieri E., Conati Barbaro C., Morandi Bonacossi D, Qasim H.A.,  
Cremaschi M. and Zerboni A. (2021) Geomorphology of the  
northwestern Kurdistan Region of Iraq: landscapes of the Zagros  
Mountains drained by the Tigris and Great Zab Rivers, *Journal of  
Maps*, 17(2), 225-236. Available  
<https://doi.org/10.1080/17445647.2021.1906339..>

Fouad, S.F. (2007) Tectonic and structural evolution. In: Geology of the  
western desert. *Iraqi journal of geology and mining*, 1, 29–50

Fouad, S.F. (2012) *Tectonic Map of Iraq, scale 1:1000000*, 3rd edition.  
Iraq Geological Survey Publications, Baghdad, Iraq.

Gilvear, D. and Bryant, R. (2016) Analysis of remotely sensed data for  
fluvial geomorphology and river science. Tools in Fluvial  
Geomorphology, John Wiley & Sons, Chichester, UK (2016), pp. 103-  
-132

Gurnell, A.M., Peiry, J.L., Petts, G.E., (2003). Using historical data in  
fluvial geomorphology. Tools in fluvial geomorphology, , John Wiley &  
Sons, Chichester 77-101.

Hasan, M., Moody, A., Benninger, L. and Hedlund H. (2019) How war,  
drought, and dam management impact water supply in the Tigris and  
Euphrates Rivers. *Ambio* 48, 264–279 Available at  
<https://doi.org/10.1007/s13280-018-1073-4>

Jassim, S.Z. and Goff, J.C. (2006) *The Geology of Iraq*, Dolin, Prague.

Kelley, J.R., Wakeley, L.D., Broadfoot, S.W., Pearson, M.L., McGrath, C.J., McGill, T.E., Jorgeson, J.D. and Talbot, C.A. (2007) Geologic setting of Mosul Dam and its engineering implications. USACE-Engineer and Development Center, Vicksburg.

Khattab, M.F. and Merkel, B.J. (2014) Application of Landsat 5 and Landsat 7 images data for water quality mapping in Mosul Dam Lake, Northern Iraq. *Arabian Journal of Geosciences*, 7(9), 3557-3573.

Available at: <https://doi.org//10.1007/s12517-013-1026-y>

Khattab, M.F., Abo, R.K., Al-Muqdadi, S.W. and Merkel, B.J. (2017) Generate reservoir depths mapping by using digital elevation model: a case study of Mosul dam lake, Northern Iraq. *Advances in Remote Sensing*, 6(3), 161-174. Available at:

<https://doi.org//10.4236/ars.2017.63012>

Koppen, W. and Geiger G., (1936) Das geographischa System der Klimate. Handbuch der Klimatologie. Gebr, Borntraeger, 1-44,

Leabi, W.K., Wanas, A.H., Nussrat, T.H., Santiago, L.M., Shukri, Z.A. and AbdulKareem, W.S. (2020) Analysis of water flow during the drought and flood seasons case study: The Mosul dam, Iraq. In IOP Conference Series: Materials Science and Engineering. IOP Publishing.

Malinowski, J. C. (2002). Iraq: A Geography, Department of Geography & Environmental Engineering, West Point.

Ministry of Water Resources (2006) Board of Expert Report No.1, On Mosul Dam Project. Baghdad, Iraq.

Mouthereau, F., Lacombe, O. and Vergés, J. (2012) Building the Zagros collisional orogen: Timing, strain distribution and the dynamics of Arabia/Eurasia plate convergence. *Tectonophysics*, 532-535, 27-60. Available at: <https://doi.org/10.1016/j.tecto.2012.01.022>

Othman, A.A. and Gloaguen, R. (2013) River courses affected by landslides and implications for hazard assessment: A high resolution remote sensing case study in NE Iraq–W Iran. *Remote sensing*. 5(3), 1024-1044. Available at: <https://doi.org/10.3390/rs5031024>

Perego, A., Zerboni, A. and Cremaschi, M. (2011) Geomorphological Map of the Messak Settafet and Mellet (central Sahara, SW Libya). *Journal of Maps*, 7(1), 464-475. Available at: <https://doi.org/10.4113/jom.2011.1207>

Saleh, D.K. (2010) Stream gage descriptions and streamflow statistics for sites in the Tigris River and Euphrates River basins, Iraq (Vol. 540). Reston, VA, USA: US Department of the Interior, US Geological Survey.

Salman, S.A., Shahid, S., Ismail, T., Ahmed, K., Chung, E.S. and Wang, X.J. (2019) Characteristics of annual and seasonal trends of rainfall and temperature in Iraq. Asia-Pacific. *Journal of Atmospheric Sciences*, 55(3), 429-438. <https://doi.org/10.1007/s13143-018-0073-4>

Sconzo, P. and Simi, F. (2020) Settlement Dynamics on the Banks of the Upper Tigris, Iraq: The Mosul Dam Reservoir Survey (1980). *Journal*

of *Open Archaeology Data*, 8(1). Available at:

<http://doi.org/10.5334/joad.63>

Sissakian, V.K. and Al-Jibouri, B.S. (2012) Stratigraphy of the low folded zone. *Iraqi Bulletin of Geology and Mining*, (5), 63-132.

Sissakian, V.K., Adamo, N. and Al-Ansari, N. (2020) The role of geological investigations for dam siting: Mosul Dam a Case Study. *Geotechnical and Geological Engineering*, 38(2), 2085-2096. Available at:

<https://doi.org//10.1007/s10706-019-01150-2>

Sissakian, V.K., Adamo, N., Al-Ansari, N., Knutsson, S., Laue, J. and Elagely, M. (2018) A comparative study of Mosul and Haditha dams, Iraq: Geological conditions. *Journal of Earth Sciences and Geotechnical Engineering*, 8(2), 35-52. Available at:

<http://urn.kb.se/resolve?urn=urn:nbn:se:ltu:diva-67809>

Sissakian, V., Al-Ansari, N. and Knutsson, S. (2014) Karstification effect on the stability of Mosul Dam and its assessment, North Iraq. *Engineering*, 6(2), 84-92. Available at:

<https://doi.org/10.4236/eng.2014.62012>

Sissakian, V.K. and Fouad, S.F. (2012) *Geological Map of Iraq, scale 1:1000000*, 4th edition. Iraq Geological Survey Publications, Baghdad, Iraq.

Sulaiman, A.H. (2016) Development of probability diagram for an observed annual rainfall in (Duhok and Sartang-Summel) Iraqi Kurdistan. 2nd scientific agricultural conference.

Tarolli, P., Cao, W., Sofia, G., Evans, D. and Ellis, E.C. (2019) From features to fingerprints: A general diagnostic framework for anthropogenic geomorphology. *Progress in Physical Geography: Earth and Environment*, 43(1), 95-128.  
<https://doi.org/10.1177/0309133318825284>

Thorndycraft, V.R., Benito, G. and Gregory, K. J. (2008) Fluvial geomorphology: A perspective on current status and methods. *Geomorphology*, 98(1-2), 2-12.

Titolo, A. (2021) Use of Time-Series NDWI to Monitor Emerging Archaeological Sites: Case Studies from Iraqi Artificial Reservoirs. *Remote Sensing* 13(4), 786. Available at:  
<https://doi.org/10.3390/rs13040786>

USGS, (1968) Declassified Corona Imaging data. Retrieved from <https://corona.cast.uark.edu> (accessed 11/08/2020).

Yamazaki, D., Ikeshima, D., Tawatari, R., Yamaguchi, T., O'Loughlin, F., Neal, J.C., Sampson, C.C., Kanae, S. and Bates, P.D. (2017) A high accuracy map of A high-accuracy map of global terrain elevations. *Geophysical Research Letters* 44(11), 5844-5853. Available at:  
<https://doi.org/10.1002/2017GL072874>

Zerboni, A., Brandolini, F., Mariani, G.S., Perego, A., Salvatori, S., Usai, D., Pelfini, M. and Williams, M.A.J. (2020) The Khartoum-Omdurman conurbation: A growing megacity at the confluence of the Blue and white Nile rivers, *Journal of Maps*, 17 (4), 227-240. Available at:  
<https://doi.org/10.1080/17445647.2020.1758810>



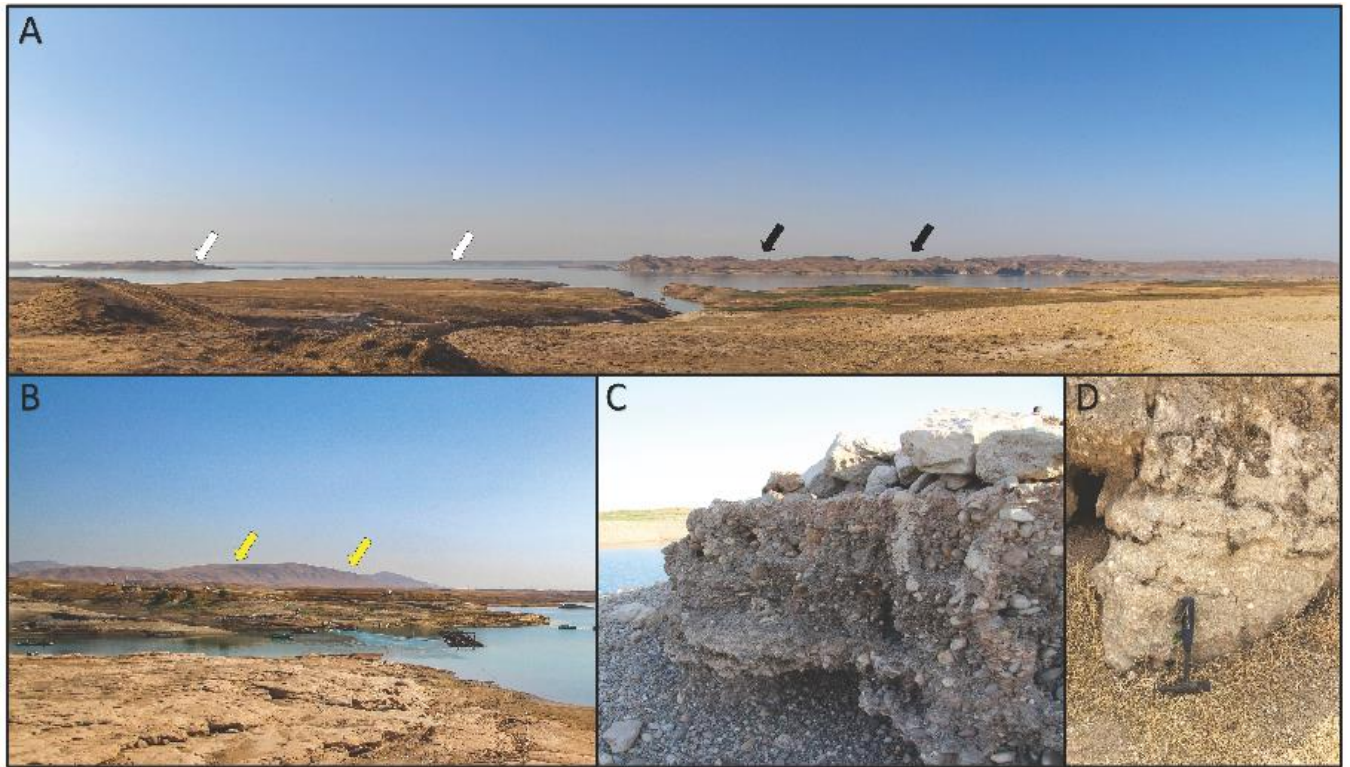


**Figure 2.** Field pictures from the MDL area. (A) Panoramic view from the left bank of MDL at a high stand in 2015; on the background the ridge of the Ravan anticline (black arrows) and the area of the dam (white arrows). (B) Panoramic view from the left bank of MDL toward East; on the background the ridge of the Dakhan anticline (yellow arrows). (C) An outcrop of the Plio- Pleistocene conglomerates close to the left bank of MDL. (D) An outcrop of the gypsum rich layers of Fathma Fm.

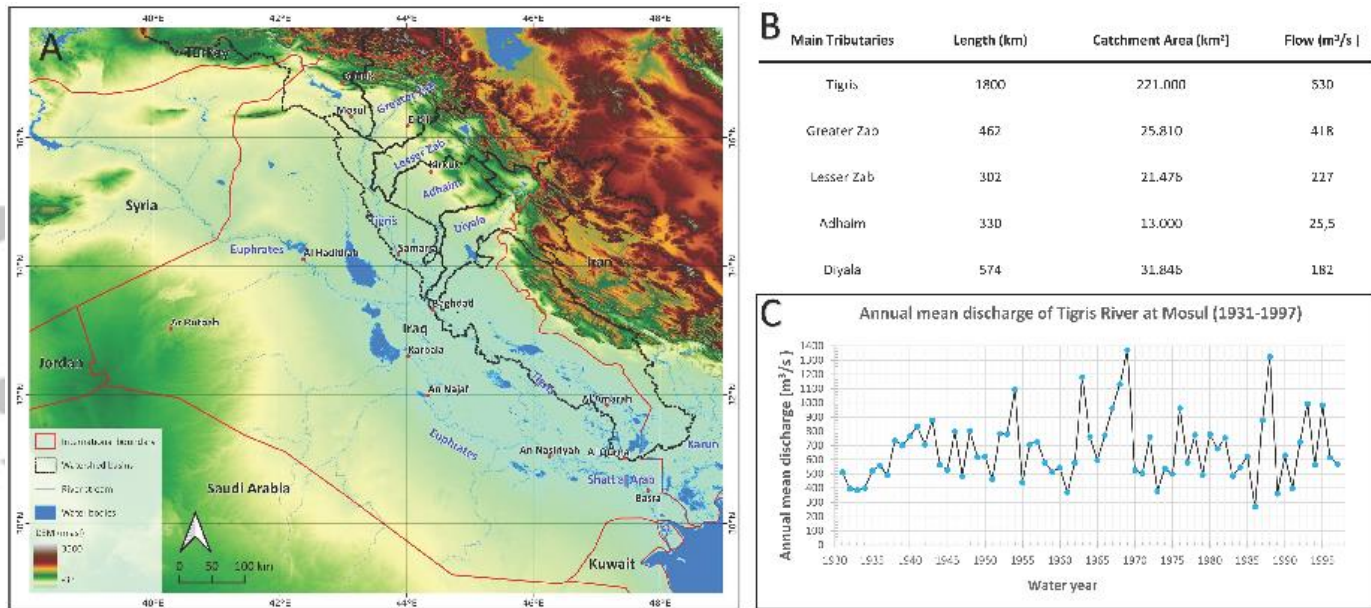


**Figure 3.** (A) Iraqi watershed basin of the Tigris River and its main tributaries extrapolated and superimposed on a MERIT DEM. (B) Information about length, catchment area and mean flow of the Tigris River and its major tributaries (Al-Ansari, 2013; ESCWA, 2013; Al-Ansari and Knutsson, 2011). (C) Annual mean discharge of the Tigris River at the Mosul stream gage derived from the USGS database (Saleh, 2010).

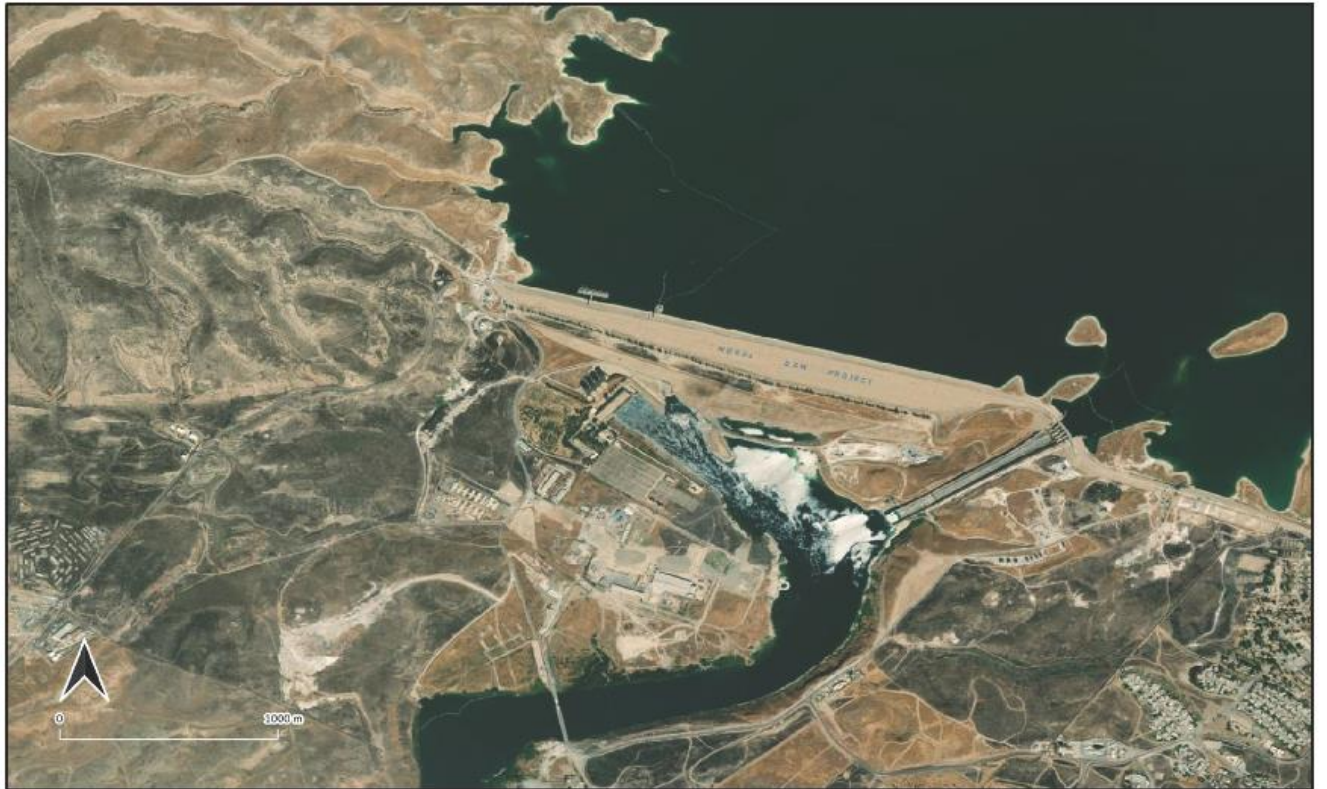


**Figure 4.** Bing Virtual Earth imagery of Mosul Dam site; notice the dam operation and the huge anthropogenic impact on the surrounding landscape.

Accepted

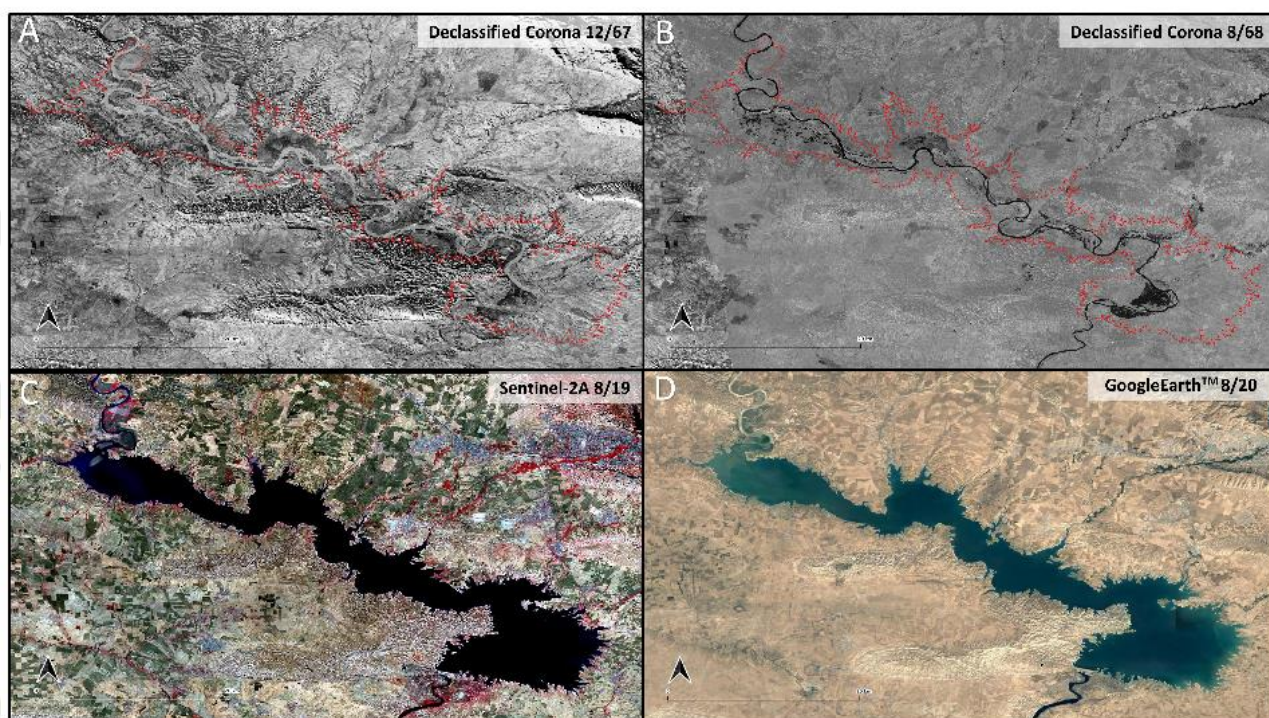


**Figure 5.** (A–B) Declassified Corona satellite images of the ancient Tigris riverscape below the MDL taken in two different phases of discharge. The red line is the current size of the MDL (C–D) Current shape of the MDL elaborated from Sentinel 2A (false colours) and Google Earth™.

Accepted





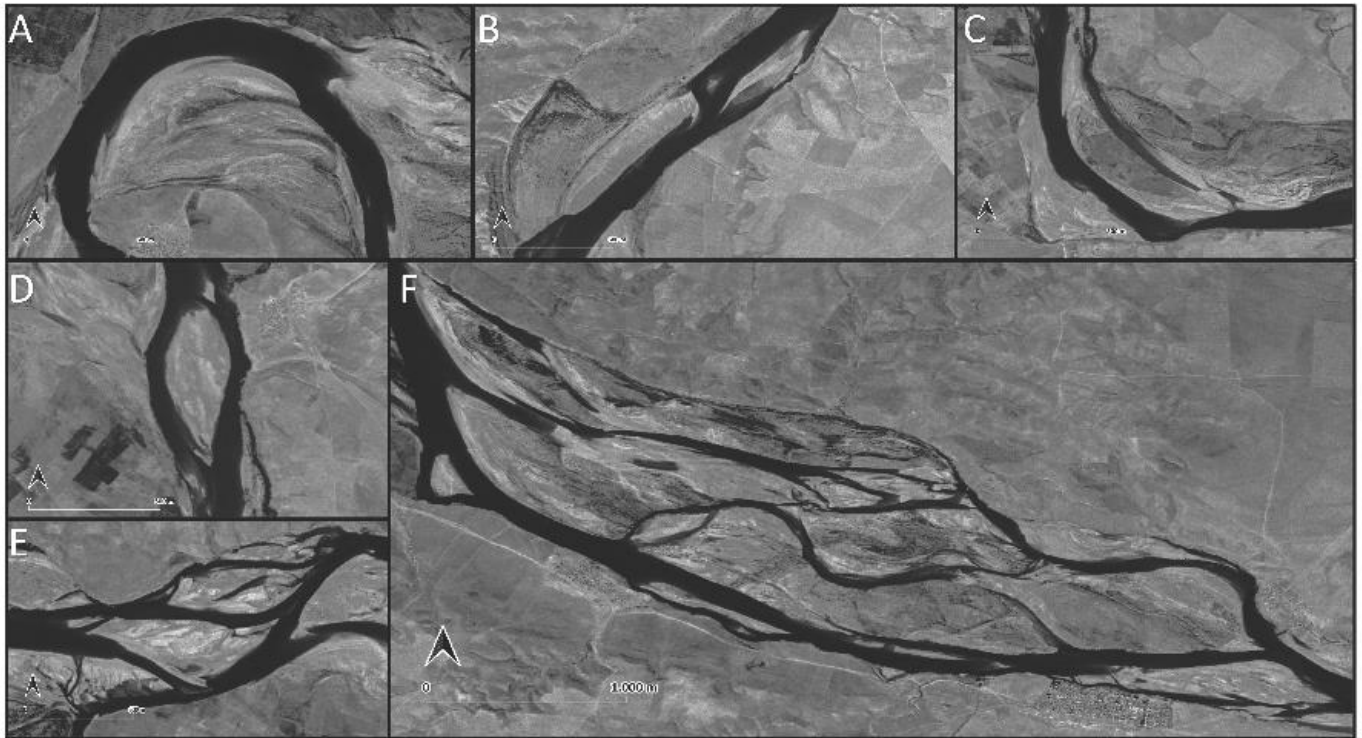


**Figure 8.** Examples of fluvial bars exposed during low flow stage derived from Declassified Corona acquired in August 1967: (A) point bar; (B-C) lateral and scroll bar; (D-E) longitudinal and diagonal bar; (F) plant-covered mid-channel islands.

Accepted

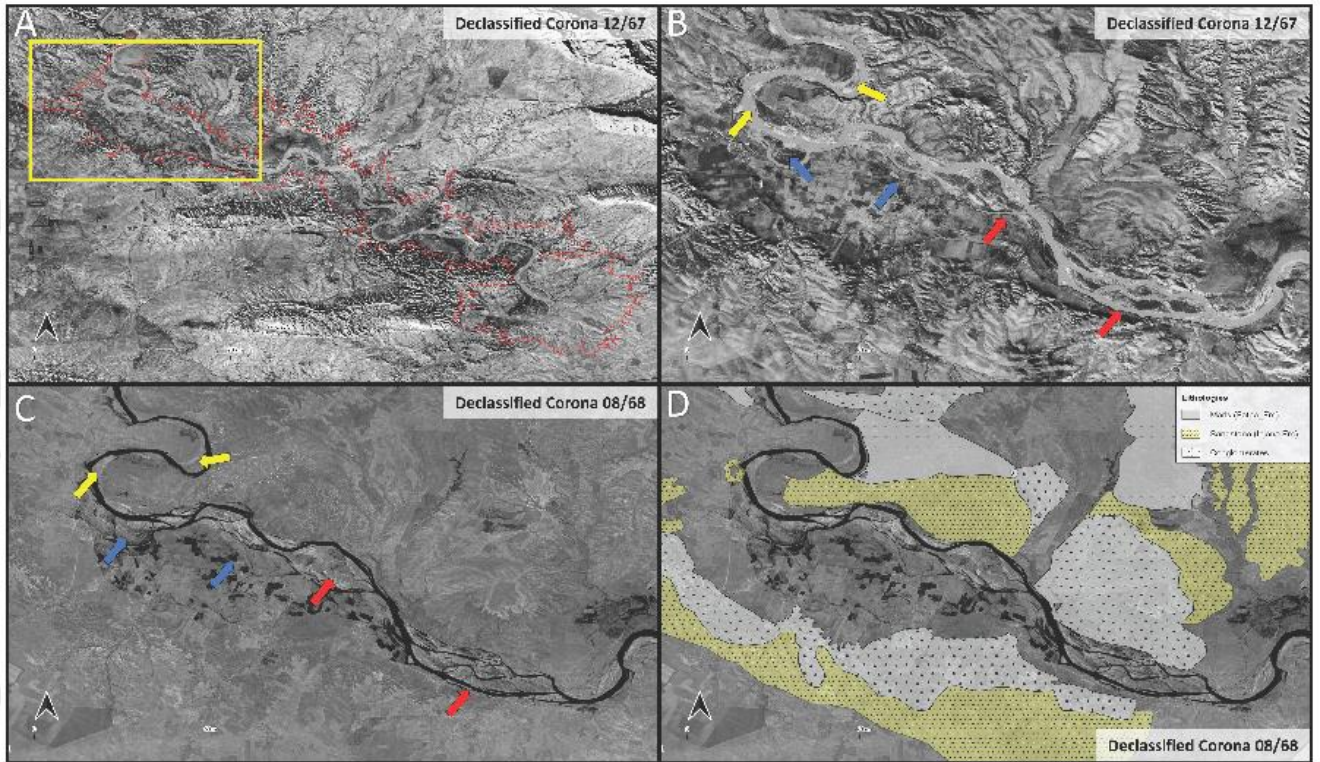


**Figure 9.** Details from the upstream sector of the river. (A) Position of the area along the Tigris River. Examples from the (B) winter and (C) summer season of the Tigris River riverbed; along the northwestern part appear tortuous meanders with small point bars (yellow arrows); then, the number of channels increases, and according to flow stage this sector shifts from wandering to anabranching with gravel bed (red arrows). The right bank hosts a large floodplain with several small fluvial features (blue arrows). (D) Lithological map of this part of the Tigris River catchment highlighting the main rock formations.

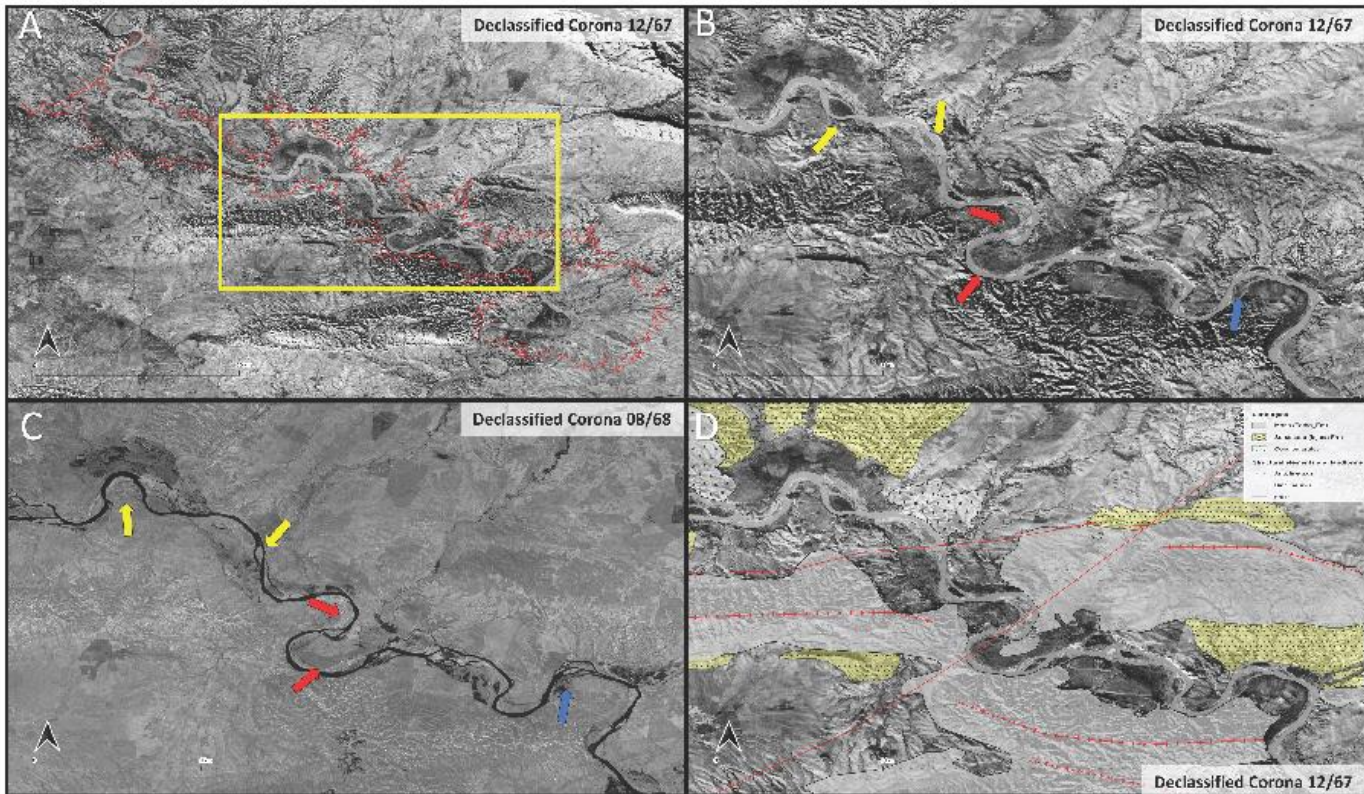


**Figure 10.** Details from the middle-stream sector of the river. (A) Position of the area along the Tigris River. Examples from the (B) winter and (C) summer season of the Tigris River riverbed showing a low sinuosity with longitudinal, lateral, and compound bars (yellow arrows). Afterwards, two tortuous meanders develop a point bar in the convex bend and a scroll bar in the concave zone (red arrows). In the lowest portion of the area, the river changes into an irregular straight planform with lateral bars (blue arrow). (D) Lithological and structural map of this part of the Tigris River catchment highlighting the litho-structural influence on the fluvial dynamic.

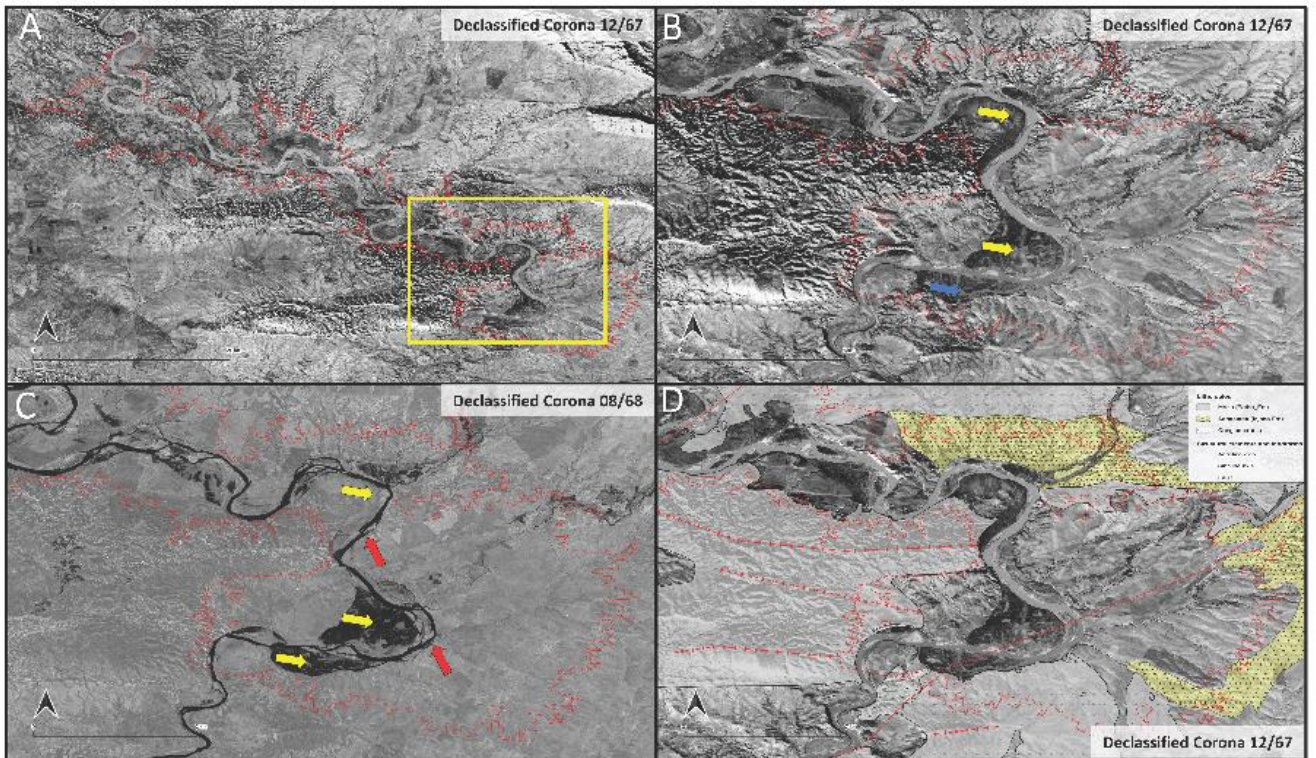


**Figure 11.** Details from the downstream sector of the river. (A) Position of the area along the Tigris River. Examples from the (B) winter and (C) summer season of the Tigris River riverbed. In this portion the river shows a tortuous planform with wide floodplains in the inner bend (yellow arrows). At the low flow stage, lateral bars and compound bars with point bars are exposed (red arrows). The floodplain located before the dam site is crossed by small secondary branches of the Tigris (blue arrow). Lithological and structural map of this part of the Tigris River catchment highlighting the influence of the anticline/syncline system and lithology on the fluvial dynamic.

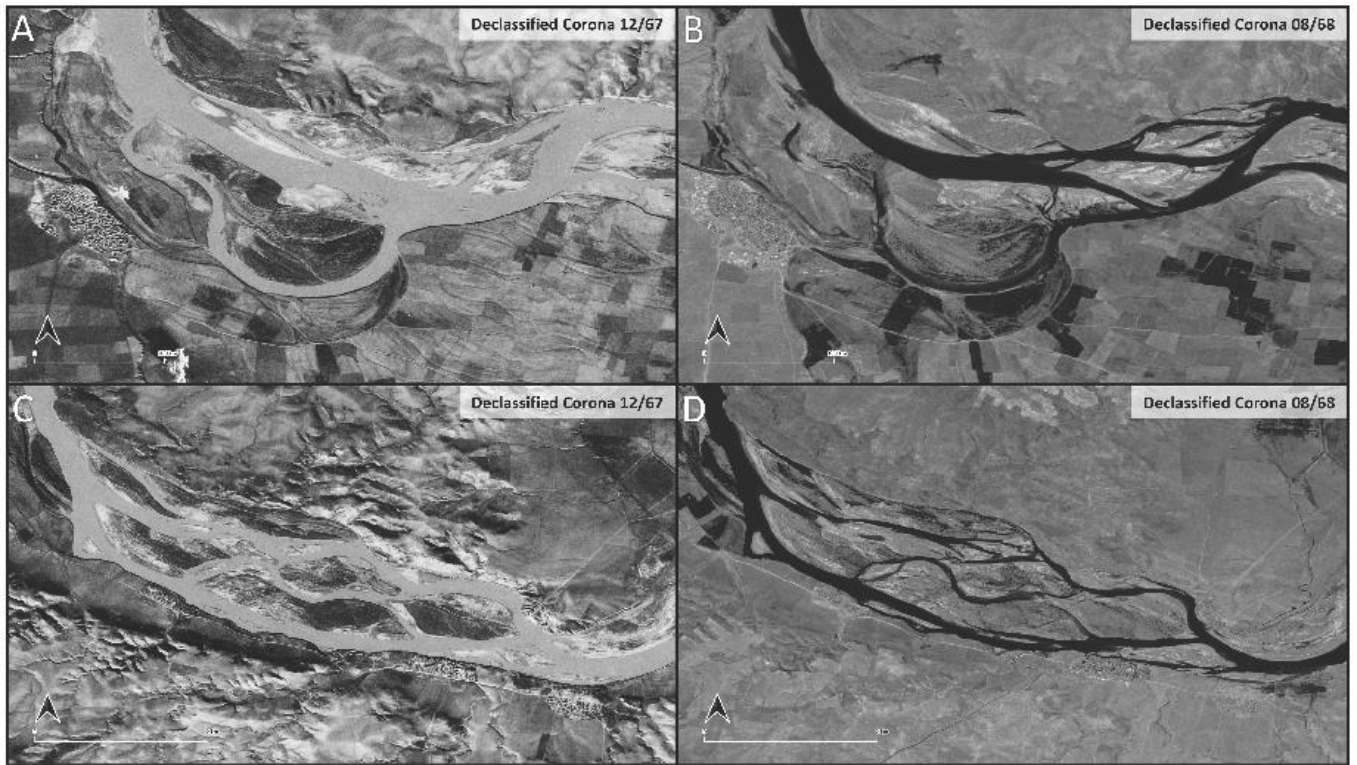


**Figure 12.** Comparison between the high and low stages of the Tigris River. (A) Large meander connected to main Tigris River channel during the bankfull stage with the formation of an island covered by vegetation and crossed by a floodchannel network. (B) In the same position as (A), meandering planform with floodplains and neck cut-off partly interconnected and filled by water during the low flow stage. (C) Wandering to (D) anabranching seasonal shift of the fluvial planform from the bankfull to the low flow stage.

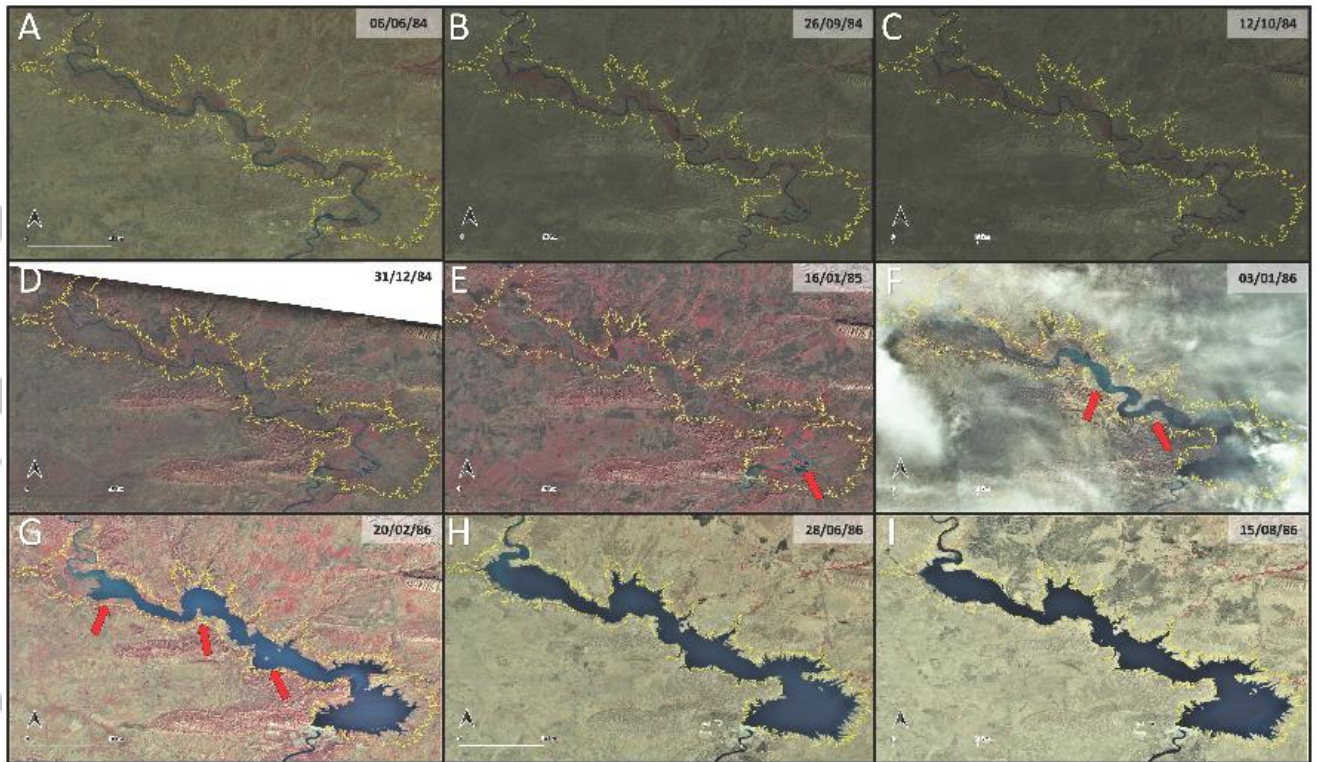


**Figure 13.** Landsat imagery (false colours) acquired during the filling phases of MDL; the yellow line is the present-day mean lake level. (A–D) Gradual embankment of the Tigris River from June to December 1984. (E) Initial inundation along the lateral unconfined setting near the dam site (red arrows). (F–G) Progressive upstream migration of the flooding, showing the inundation of the meandering area and the floodplain in the partly laterally confined valley (red arrows). (H–I) Final stages of filling of the MDL in the summer of 1986; the basin shape corresponds to the current one.

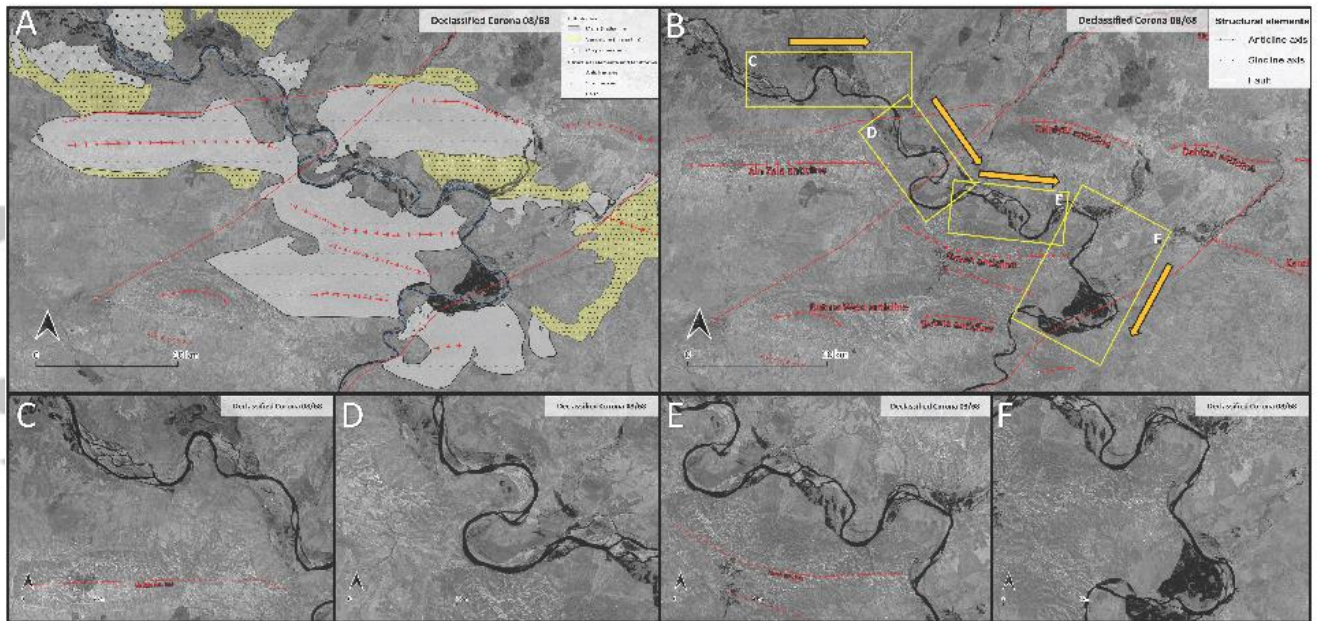


**Figure 14.** (A) Structural and lithological setting of the study area. (B) Division of the Tigris River into four sections corresponding to main planform and flow direction shifts. (C) Particular of the Tigris flowing W–E parallel to the strike direction of the Ain Zala Anticline. (D) Tortuous meanders and NW–SE shifting of the Tigris River. (E) Subsequent changes toward W–E following the growth of the Ravan Anticline. (F) Irregular meandering pattern and direction shift toward NE–SW in the downstream portion of the river, due to the combined influence of the Dohuk Fault System and the syncline subsidence.

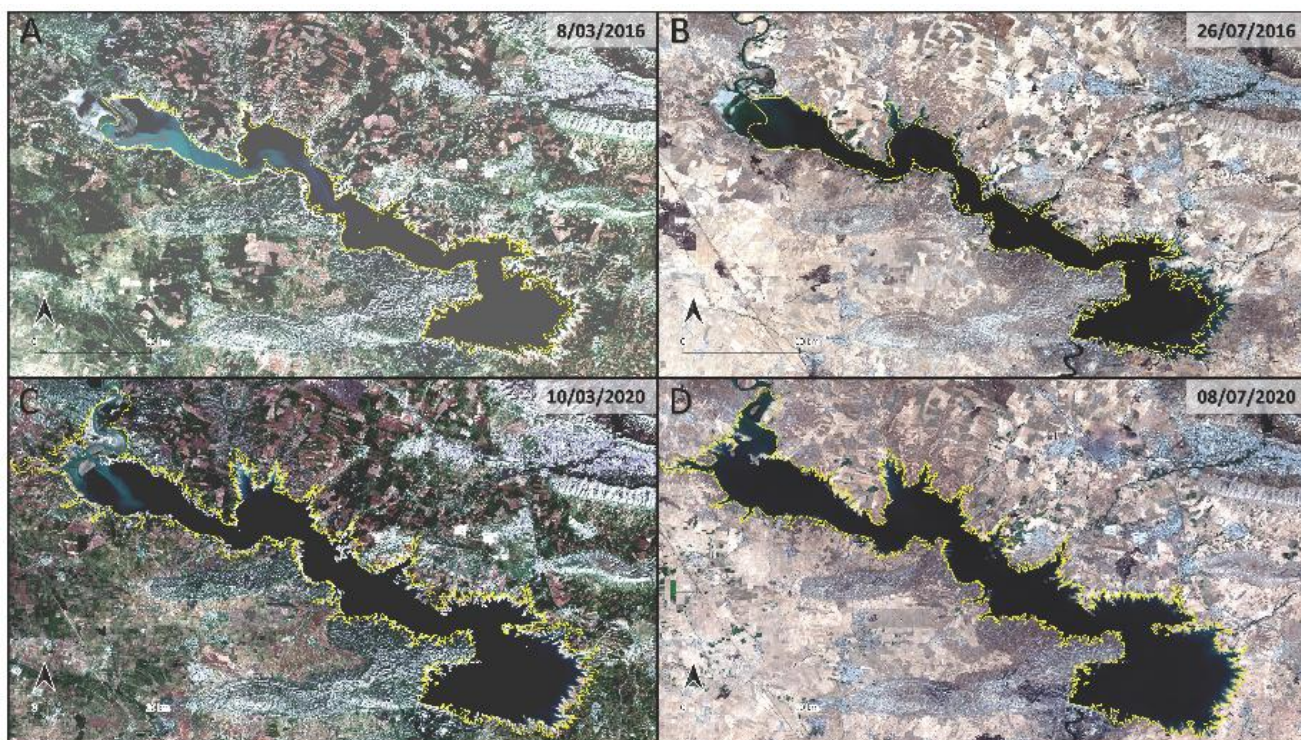


**Figure 15.** Recent dam operations triggering variations of the MDL water level and its shoreline captured by Sentinel-2 satellite imagery (false colours); lake level variations are also controlled by seasonal changes in fluvial discharge. (A-B) March-July 2016; (C-D) March-July 2020.

Accepted

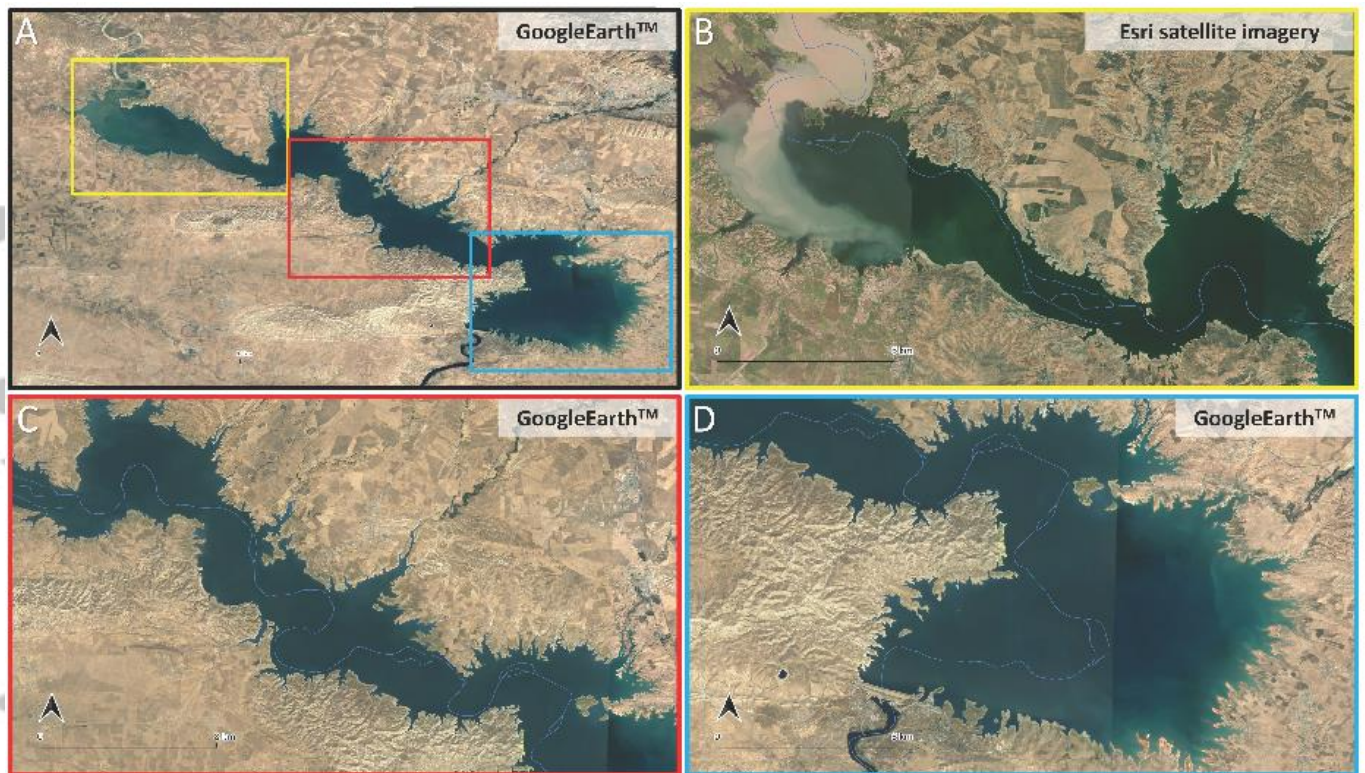


**Figure 16.** (A) Different portions of the MDL basin as discussed in the text: upstream (yellow box), middle stream (red box) and downstream (blue box); the submerged Tigris River stream is outlined in light blue. (B) The overprint of a submerged meander planform controls the aspect of the basin and shoreline in the upstream portion, also influencing the inlet of the Tigris River into the lake; this is highlighted by the curved shape of the deltaic plume. Afterwards, the narrowing of the lake is controlled by the presence of the confined Tigris River valley (canyon) cut into the Plio-Pleistocene conglomerates, indicating a strong lithological control. (C) The central part of the MDL (middle stream) is characterized by a partly straight partly arcuate coastline profile on the right banks, which are influenced by the complex structural setting of the area that alternates faults and folds. (D) At the dam site, the reservoir reaches the maximum surface expansion

by occupying the wide flat depression produced by the interplay between the syncline/anticline system and the Dohuk Fault System.

Accepted Article

Dataset	Name	Period	Ground Resolution	Monthly mean Discharge(m3/s) (MOS)
Declassified Corona Image	ds1102-1025df006	11/12/1967	6 feet	481,4
Declassified Corona Image	ds1102-1025df007	11/12/1967	6 feet	
Declassified Corona Image	ds1102-1025df008	11/12/1967	6 feet	
Declassified Corona Image	ds1102-1025df010	11/12/1967	6 feet	
Declassified Corona Image	ds1102-1025df015	11/12/1967	6 feet	
Declassified Corona Image	ds1102-1025df016	11/12/1967	6 feet	
Declassified Corona Image	ds1104-2138da003	16/08/1968	6 feet	211,6
Declassified Corona Image	ds1104-2138da004	16/08/1968	6 feet	
Declassified Corona Image	ds1104-2138da005	16/08/1968	6 feet	
Declassified Corona Image	ds1104-2138da006	16/08/1968	6 feet	
Declassified Corona Image	ds1104-2138da007	16/08/1968	6 feet	
Landsat 4-5 Thematic Mapper	LT05_L1TP_170034_19840606	06/06/1984	30 m	535,4
Landsat 4-5 Thematic Mapper	LT05_L1TP_170035_19840606	06/06/1984	30m	
Landsat 4-5 Thematic Mapper	LT05_L1TP_170034_19840926	26/09/1984	30 m	118
Landsat 4-5 Thematic Mapper	LT05_L1TP_170035_19840926	26/09/1984	30 m	
Landsat 4-5 Thematic Mapper	LT05_L1TP_170034_19841012	12/10/1984	30 m	191,1
Landsat 4-5 Thematic Mapper	LT05_L1TP_170035_19841231	13/12/1984	30 m	659,3
Landsat 4-5 Thematic Mapper	LT05_L1TP_170034_19850116	16/01/1985	30m	350,6
Landsat 4-5 Thematic Mapper	LT05_L1TP_170035_19850116	16/01/1985	30m	
Landsat 4-5 Thematic Mapper	LT05_L1GS_170034_19860103	03/01/1986	30 m	92,1
Landsat 4-5 Thematic Mapper	LT05_L1GS_170035_19860103	03/01/1986	30m	
Landsat 4-5 Thematic Mapper	LT05_L1TP_170034_19860220	20/02/1986	30 m	102,5
Landsat 4-5 Thematic Mapper	LT05_L1TP_170035_19860220	20/02/1986	30 m	
Landsat 4-5 Thematic Mapper	LT05_L1TP_170034_19860815	15/05/1986	30 m	553,5
Landsat 4-5 Thematic Mapper	LT05_L1TP_170034_19860628	28/06/1986	30 m	503,1
Landsat 4-5 Thematic Mapper	LT05_L1TP_170035_19860628	28/06/1986	30 m	
Landsat 4-5 Thematic Mapper	LT05_L1TP_170035_19860815	15/08/1986	30 m	296,5
Sentinel-2	S2A_OPER_MSI_L1C_TL_MTI_20160308T080055_20160308T115917_A003707_T38SKF_NO2_01_01	08/03/2016	10 m	
Sentinel-2	S2A_OPER_MSI_L1C_TL_MTI_20160308T080055_20160308T115917_A003707_T38SLF_NO2_01_01	08/03/2016	10 m	
Sentinel-2	L1C_T38SKF_A005709_20160726T075850	26/07/2016	10 m	
Sentinel-2	L1C_T38SLF_A005709_20160726T075850	26/07/2016	10 m	
Sentinel-2	S2B_MSIL2A_20191108T080029_N0213_R035_T38SKF	11/08/2019	10 m	
Sentinel-2	S2A_MSIL2A_20191108T075131_N0213_R135_T38SLF_	11/08/2019	10 m	
Sentinel-2	L1C_T38SKF_A024628_20200310T080339	10/03/2020	10 m	
Sentinel-2	L1C_T38SLF_A024628_20200310T080339	10/03/2020	10 m	
Sentinel-2	L1C_T375GA_A026344_20200708T080203	08/07/2020	10 m	
Sentinel-2	L1C_T375GA_A026344_20200708T080203	08/07/2020	10 m	
Sentinel-2	L1C_T38SLF_A026301_20200705T075705	08/07/2020	10 m	

**Table 1.** Database of satellite imagery used in this work; the monthly discharge of the Tigris River is reported when available.

Graphical abstract

**Declassified intelligence satellite imagery as a tool to reconstruct past landforms and surface processes. The submerged riverscape of the Tigris River below the Mosul Dam Lake, Iraq**

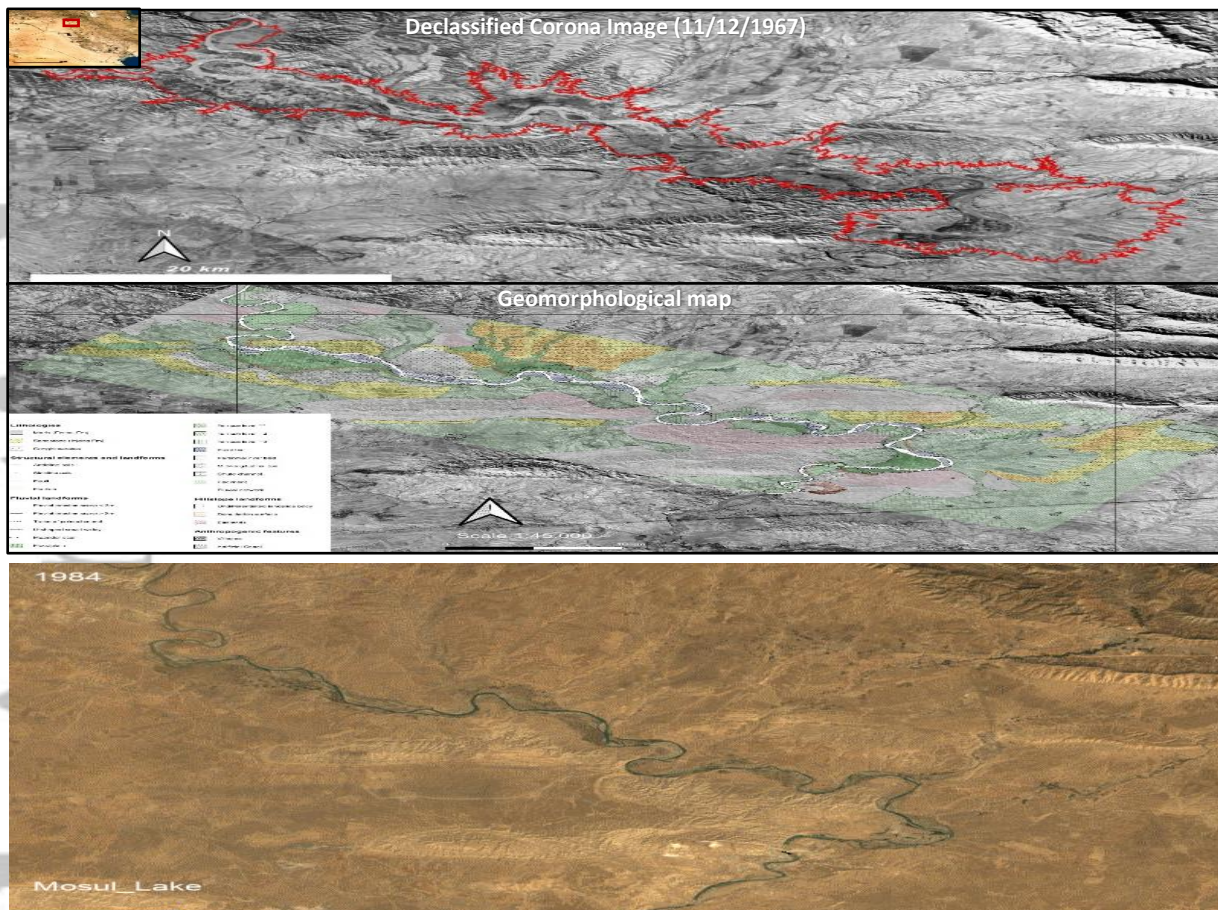
Luca Forti<sup>1,2\*</sup>, Guido S. Mariani<sup>3</sup>, Filippo Brandolini<sup>4</sup>, Andrea Pezzotta<sup>1</sup>,  
Andrea Zerboni<sup>1</sup>

*1) Dipartimento di Scienze della Terra "A. Desio", Università degli Studi di Milano, via L. Mangiagalli 34, I-20133 Milano, Italy.*

*2) Istituto di Geoscienze e Georisorse, Consiglio Nazionale delle Ricerche, Via G. Moruzzi 1, 56124 Pisa, Italy.*

*3) Dipartimento di Scienze Chimiche e Geologiche, Università degli Studi di Cagliari, Italy.*

*4) McCord Centre for Landscape - School of History, Classics and Archaeology Newcastle University, Armstrong Building, Newcastle upon Tyne - NE17RU (UK)*



Accepted